

# The effects of natural gas composition on conventional dual-fuel and reactivity-controlled compression ignition combustion in a heavy-duty diesel engine

International J of Engine Research

2022, Vol. 23(3) 397–415

© IMechE 2021



Article reuse guidelines:

[sagepub.com/journals-permissions](https://sagepub.com/journals-permissions)

DOI: 10.1177/1468087420984044

[journals.sagepub.com/home/ijer](https://journals.sagepub.com/home/ijer)

Vinicius B Pedrozo<sup>ID</sup>, Xinyan Wang<sup>ID</sup>, Wei Guan and Hua Zhao

## Abstract

The use of natural gas (NG) in dual-fuel heavy-duty engines has the potential to reduce pollutant and greenhouse gas (GHG) emissions from the transport sector when compared to the conventional diesel engines. However, NG composition and methane slip are of interest because both can adversely affect the benefits of NG as an alternative fuel, especially when considering GHG emissions. Therefore, this study experimentally investigated the effects of NG fuel properties on the performance and emissions of both conventional dual-fuel and reactivity-controlled compression ignition (RCCI) engine operations. Three different gas mixtures were selected to simulate typical NG compositions available in the world market, with methane numbers (MN) of 80.9, 87.6 and 94.1. These fuels were tested in a single-cylinder compression ignition engine operating at 0.6, 1.2 and 1.8 MPa net indicated mean effective pressure (IMEP). A high-pressure common rail system allowed for the use of various diesel injection strategies while a variable valve actuation system enabled the effective compression ratio to be adjusted via late intake valve closing (LIVC). The RCCI combustion was found to be more sensitive to changes in MN than the conventional NG-diesel dual-fuel operation. The gas mixture with the lowest MN reduced both total unburned hydrocarbons emissions and methane slip at the expense of higher nitrogen oxides (NO<sub>x</sub>) emissions. The effects of MN on the net indicated efficiency were more significant at 0.6 MPa IMEP, yielding differences of up to 4.9% between the RCCI operations with the lowest and highest MN fuels. Overall, this work revealed that the combination of the RCCI combustion and LIVC can achieve up to 80% lower methane slip and NO<sub>x</sub> emissions and relatively higher net indicated efficiency than the conventional dual-fuel regime, independent of the NG composition.

## Keywords

Natural gas, CNG, LNG, methane number, methane slip, dual-fuel, diesel engine, RCCI, combustion

Date received: 25 October 2020; accepted: 3 December 2020

## Highlights

- Three NG compositions were evaluated in conventional dual-fuel and RCCI combustion modes.
- RCCI combustion was more sensitive to changes in methane number.
- LIVC strategy helps to adjust in-cylinder lambda and minimise methane slip.
- Lower CH<sub>4</sub> and NO<sub>x</sub> emissions and higher efficiency on RCCI mode.

## Introduction

Natural gas (NG), either compressed or liquefied, is an attractive substitute for gasoline and diesel in the

transportation sector due to its relatively lower carbon footprint and competitive cost per unit of energy.<sup>1</sup> However, the use of NG in naturally aspirated spark ignition (SI) engines can decrease the peak torque and power due to a reduction in volumetric efficiency when compared to a counterpart gasoline SI engine.<sup>2</sup> Turbocharged SI engines could potentially minimise these effects and take advantage of the high knock

Centre for Advanced Powertrain and Fuels, Brunel University London, Uxbridge, UK

### Corresponding author:

Vinicius B Pedrozo, Centre for Advanced Powertrain and Fuels, Brunel University London, Kingston Lane, Uxbridge, Middlesex UB8 3PH, UK.  
Email: [pedrozo.vinicius@gmail.com](mailto:pedrozo.vinicius@gmail.com)

**Table 1.** Euro VI emissions limits for Type 2B heavy-duty dual-fuel engines.

Emission	Unit	WHSC	WHTC ( $GER_{WHTC} \leq 68\%$ )	WHTC ( $GER_{WHTC} > 68\%$ )
Nitrogen oxides (NO <sub>x</sub> )	g/kWh	0.40	0.46	0.46
Carbon monoxide (CO)	g/kWh	1.50	4.00	4.00
Particulate matter (PM)	g/kWh	0.01	0.01	0.01
Total unburned hydrocarbon (THC)	g/kWh	0.13	$0.16 + 0.50 GER_{WHTC}$	—
Non-methane hydrocarbon (NMHC)	g/kWh	—	—	0.16
Methane (CH <sub>4</sub> )	g/kWh	—	—	0.50

resistance of NG but the overall engine cost might not be competitive. Moreover, the use of NG in a lean combustion system is challenging due to reduced mixture flammability, resulting in poor fuel conversion efficiency. This results in the need for a relatively expensive and complex aftertreatment system, which can no longer rely exclusively on a three-way catalyst.<sup>3</sup> However, lean NG-diesel dual-fuel compression ignition combustion have been demonstrated as an effective means of utilising NG and potentially lowering the total cost of ownership of heavy-duty vehicles.<sup>4</sup>

In a dual-fuel compression ignition engine, NG can be supplied through port fuel injection (PFI) system to ensure a lean and homogeneous distribution of the low reactivity fuel in the combustion chamber prior to ignition and combustion. The high reactivity diesel fuel is directly injected into the combustion chamber to create multiple ignition sites.<sup>5</sup> This strategy enables reductions in local fuel/air equivalence ratio and combustion temperatures when compared to a diesel-only operation, minimising soot and NO<sub>x</sub> formation.<sup>6</sup> Additionally, dual-fuel compression ignition engines present lower pumping and heat transfer losses than stoichiometric SI engines, allowing for higher fuel conversion efficiency.

The benefits of an NG-diesel dual-fuel combustion, however, are often accompanied with unburned methane (CH<sub>4</sub>) emissions, also known as methane slip. According to the Intergovernmental Panel on Climate Change (IPCC),<sup>7</sup> CH<sub>4</sub> is a GHG with 28 times higher global warming potential (GWP) than carbon dioxide (CO<sub>2</sub>) emissions over a 100-year lifetime. This increases the relative impact of unburned CH<sub>4</sub> emissions on climate change.<sup>8</sup> To demonstrate this adverse effect, Stettler et al.<sup>9</sup> analysed the energy consumption, GHG emissions and pollutants from five after-market dual-fuel engine configurations in two vehicle platforms. They reported that over a transient cycle, lean-burn NG fuelled vehicles reduced CO<sub>2</sub> emissions by up to 9% when compared to the diesel-only baseline. However, CH<sub>4</sub> emissions from incomplete combustion increased the GHG emissions by 50%–127% relative to the equivalent diesel engine vehicle.

To control the pollutant and GHG emissions of dual-fuel combustion engines, the Regulation No. 49 of the Economic Commission for Europe of the United Nations (UN/ECE)<sup>10</sup> complements the Euro VI

emissions standards for on-road heavy-duty vehicles<sup>11,12</sup> and establishes five different types of dual-fuel engines. For the sake of brevity, this research work will be focused on the analysis of Type 2B heavy-duty dual-fuel (HDDF) engines. These operate over the hot part of the World Harmonized Transient Driving Cycle (WHTC) with an average gas energy ratio ( $GER_{WHTC}$ ) between 10% and 90% while maintaining the possibility of a diesel-only engine operation.

Displayed in Table 1 are the Euro VI emissions limits for Type 2B HDDF engines over the stationary (WHSC) and transient (WHTC) test cycles. Hydrocarbon emissions limit under the WHTC will vary depending on the  $GER_{WHTC}$ . If the  $GER_{WHTC}$  is higher than 68%, the engine can operate with slightly less stringent limits as indicated by the sum of non-methane hydrocarbon (NMHC) and CH<sub>4</sub> emissions. Nevertheless, CH<sub>4</sub> emissions should be controlled at less than 0.5 g/kWh. Achieving this target is particularly challenging because of the stability of the CH<sub>4</sub>,<sup>13</sup> which is the predominant constituent of NG.<sup>14</sup> Additionally, low exhaust gas temperatures observed during the WHTC might not allow the methane oxidation catalyst (MOC) to reach the light-off temperature quickly enough, increasing the levels of methane slip.<sup>1</sup>

The limits shown in Table 1 indicate that a NG-diesel dual-fuel engine needs to be highly optimised to curb engine-out CH<sub>4</sub> emissions. A potential solution is to modify the characteristics of the in-cylinder heat release rate depending on the dual-fuel engine operating conditions, such as load, speed and working temperatures.<sup>15</sup> The first strategy (Mode A) does not require NG and typically employs a single diesel injection near firing top dead centre (TDC). This strategy represents the conventional diesel combustion (CDC) and can be used for cold starting and idling the engine. A pilot and a post diesel injection may be applied if necessary.<sup>16,17</sup>

The second engine operation strategy (Mode B) is a conventional dual-fuel combustion process.<sup>18</sup> This dual-fuel regime uses a relatively late diesel injection, with or without a pre-injection, to provide the ignition source for the premixed charge of NG and air. The amount of energy supplied by the diesel fuel can be as low as 3%.<sup>19</sup> However, the use of high NG energy fractions via a conventional PFI system can potentially lead to excessive engine-out CH<sub>4</sub> emissions, decreasing

the fuel conversion efficiency and the competitiveness of the dual-fuel combustion over the CDC operation in Mode A.<sup>20</sup>

The third heat release strategy (Mode C) consists of a more premixed dual-fuel combustion process, often referred to as RCCI combustion.<sup>5</sup> This dual-fuel regime is typically achieved by using an early single diesel injection,<sup>21,22</sup> early split diesel injections<sup>21,22</sup> or late split diesel injections.<sup>4</sup> After a relatively longer ignition delay, multiple compression ignition points initiate the combustion which sequentially progresses from high reactivity to low reactivity zones.<sup>23,24</sup> This helps to increase the temperature and flammability of the premixed charge,<sup>25</sup> promoting a more uniform burning and decreasing CH<sub>4</sub> emissions.<sup>26</sup> Previous studies have shown that Mode C yields higher fuel conversion efficiency and lower THC and NO<sub>x</sub> emissions than a dual-fuel operation in Mode B.<sup>27</sup> However, RCCI can have a limited operating range over the engine speed-load map due to peak in-cylinder pressure and pressure rise rate limitations.<sup>28–30</sup>

Besides the diesel injection strategy, the properties of the low reactivity fuel have a major impact on the dual-fuel combustion process and influence both engine performance and emissions.<sup>31</sup> In the case of NG-diesel dual-fuel engines, these effects are generally driven by the gas composition, which can vary significantly with the source of supply and production process.<sup>14,32</sup> Moreover, the composition and the resulting properties of liquefied natural gas (LNG) are susceptible to changes during storage arising from the evaporation of lighter components (e.g. boil-off).<sup>33,34</sup>

Major NG properties that define its quality are the energy density and knock resistance. The NG energy density is usually given by the Wobbe index (WI), which indicates the fuel interchangeability.<sup>35</sup> WI can be calculated as the ratio of the higher heating value (HHV) per unit of volume and the square root of the relative density under the same reference condition.<sup>10,36</sup> Moreover, the resistance of an NG fuel to engine knocking is described by the methane number (MN), which can be calculated by different empirical methods based on actual engine measurements.<sup>34,36</sup> Unfortunately, there is currently not a single commonly used method for calculating the MN of NG fuels.<sup>37,38</sup> Nevertheless, it is well known that higher hydrocarbons, such as ethane (C<sub>2</sub>H<sub>6</sub>) and propane (C<sub>3</sub>H<sub>8</sub>), have lower knock resistances than CH<sub>4</sub><sup>39</sup> which can accelerate compression ignition of the NG fuel and thus decrease its MN.<sup>40</sup> The opposite is true for an NG mixture containing a higher concentration of inert gases such as CO<sub>2</sub> and nitrogen (N<sub>2</sub>).<sup>37</sup>

Extensive studies on the influence of NG quality have been performed on SI engines, demonstrating that NG fuels with lower MN can reduce CH<sub>4</sub> emissions<sup>32,41</sup> at the expense of lower engine efficiency.<sup>42,43</sup> However, there is limited research focused on the effects of the gas composition on NG-diesel dual-fuel engines, particularly in the more sensitive

RCCI combustion governed by chemical kinetics.<sup>44</sup> One of the few studies was performed by Van Alstine et al.,<sup>45</sup> where engine experiments were combined with computational fluid dynamics (CFD) simulations to evaluate the influence of MN on conventional dual-fuel combustion characteristics. Part load results for 10 different NG compositions showed that the method selected for the calculation of MN (referred to as MWM) did not correlate well with the propensity for rapid heat release occurring near the end of the combustion event.

Wu et al.<sup>46</sup> performed CFD simulations of the effects of MN on both conventional dual-fuel and RCCI combustion at a medium engine load. Surprisingly, the authors reported that the combustion and thermal efficiencies of an RCCI operation were not sensitive to variations in the NG composition. Finally, Kakae et al.<sup>47</sup> assessed the impact of WI on RCCI combustion using CFD studies. Mid-load results demonstrated that an NG composition with a higher WI (and a lower MN) can decrease THC and CO emissions via higher peak in-cylinder pressures and temperatures. Overall, the analysis of previous studies demonstrated that the existing understanding of the effects of NG quality on dual-fuel combustion has to be broadened. It is necessary to elucidate the influence of NG composition over a wide range of engine load conditions, focusing on both conventional dual-fuel (Mode B) and RCCI (Mode C) operations.

The current lack of an experimental comparison showing the impacts of NG quality on different dual-fuel combustion modes hinders the development of high-efficiency and clean dual-fuel engines. Therefore, the present work seeks to better understand the effects of NG composition on the combustion, emissions and fuel conversion efficiency of conventional dual-fuel and RCCI operations at three engine loads. The experiments were conducted with three gas mixtures of different MN in a single-cylinder diesel engine. Advanced combustion control strategies, such as multiple diesel injections and late intake valve closing (LIVC) have been explored. The results of this research work are expected to guide the optimisation of multi-cylinder dual-fuel engine calibration as well as help mitigate climate forcing pollutants, such as CH<sub>4</sub> and CO<sub>2</sub> emissions.

## Experimental setup

### *Experimental facilities and engine specifications*

A schematic diagram of the single-cylinder compression ignition engine experimental setup is depicted in Figure 1. An eddy current dynamometer was used to absorb the power produced by the engine. Fresh intake air was supplied to the engine via an external compressor with closed-loop control for the boost pressure. A throttle valve located upstream of a surge tank provided fine control over the intake manifold

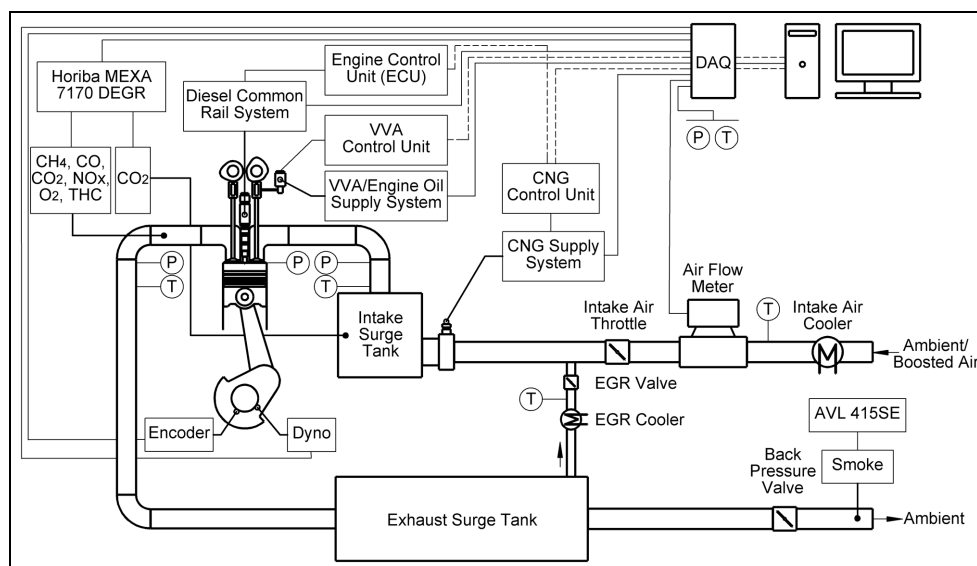


Figure 1. Schematic diagram of the dual-fuel engine experimental setup.

Table 2. Single cylinder HD engine specifications.

Parameter	Value
Bore/stroke	129/155 mm
Connecting rod length	256 mm
Swept volume	2.026 dm <sup>3</sup>
Geometric compression ratio	16.8
Maximum in-cylinder pressure	18 MPa
Piston type	Re-entrant bowl
Diesel injection system	Bosch common rail, injection pressure of 30–220 MPa, 8 holes, 150° spray
NG port fuel injection system	G-Volution controller and two clean air power injectors SP-010, injection pressure of 800 kPa

pressure. The air mass flow rate ( $\dot{m}_{air}$ ) was measured with a thermal mass flow meter. The temperature of the boosted air was controlled using a water-cooled heat exchanger. Another surge tank was installed in the exhaust manifold to damp out pressure fluctuations. An electronically controlled backpressure valve located downstream of the exhaust surge tank was used to set the required exhaust manifold pressure.

The heavy-duty (HD) engine hardware specifications are outlined in Table 2. The combustion system consisted of a 4-valve swirl-oriented cylinder head and a stepped-lip piston bowl design. Coolant and oil pumps were driven by separate electric motors. Engine coolant and oil temperatures were set to 85°C. The oil pressure was held at 450 kPa throughout the experiments.

Besides, the engine is equipped with a prototype lost-motion variable valve actuation (VVA) system on the intake camshaft. The system incorporates a

hydraulic collapsing tappet on the valve side of the rocker arm, enabling the adjustment of the intake valve closing (IVC) via a normally open high-speed solenoid valve assembly and a special intake cam design. This allows for a Miller cycle operation via LIVC,<sup>48,49</sup> which helps to improve upon the work extraction potential from over-expansion.<sup>50</sup> This is achieved via a reduction in the effective compression ratio (ECR), which decreases the compression pressures and temperatures as well as the in-cylinder mass trapped at a given boost pressure.

The intake valve lift curves employed in this study are depicted in Figure 2. The intake valve opening (IVO) was held constant at  $-354 \pm 1$  crank angle degrees (CAD) after firing top dead centre (ATDC), as determined at 0.5 mm valve lift. The relatively late IVO was used to minimise the scavenging effects and thus the chances of having CH<sub>4</sub> short-circuiting the combustion chamber via positive valve overlap.<sup>4</sup> The IVC was moved from  $-157 \pm 1$  CAD ATDC in the conventional dual-fuel cases to a preselected IVC at  $-97 \pm 1$  CAD ATDC in the RCCI cases with LIVC lowering the ECR from 16.8 to 13.8. To better account for the flow resistance across the intake valves<sup>51</sup> and inertia of the gas in the intake port before the inlet valves are closed,<sup>52</sup> a pressure-based ECR was used as a reference. Therefore, the ECR was calculated as

$$ECR = \frac{V_{cyl @ effective IVC}}{V_{cyl @ TDC}}$$

where  $V_{cyl @ effective IVC}$  is the in-cylinder volume at the effective IVC, which was obtained from the intersection of the average intake manifold pressure and an extrapolated polytropic compression curve fitted to the

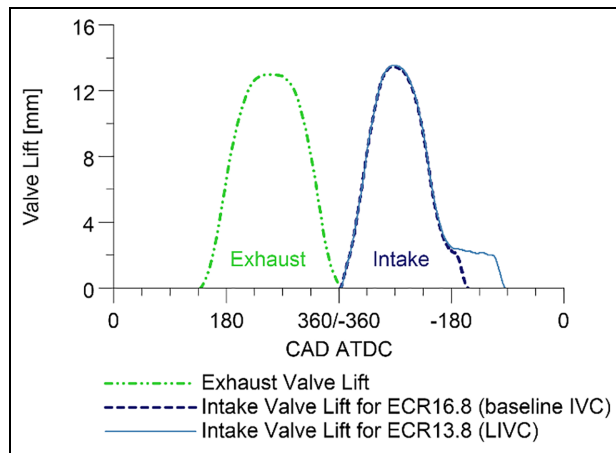


**Figure 2.** Overview of the fixed exhaust valve lift and variable intake valve lift curves used in this study.

experimental in-cylinder pressure;<sup>51,53</sup> and  $V_{cyl@TDC}$  is the clearance volume at TDC.

### Fuel supply

The NG fuel was stored in a rack of six interconnected 15 MPa bottles outside of the engine test cell. Specially developed hoses for the conveyance of NG have been used, as they are constructed of an electrically conductive nylon core designed to dissipate static build-up. From there, the NG was fed into a pair of pneumatically controlled safety valves, a high-pressure filter and a high-pressure regulator that dropped the gas pressure to 1 MPa. The pressure regulator was water-cooled to counteract the reduction in temperature experienced by the gas during expansion.

After the high-pressure regulator, the NG was brought inside the test cell and into an Endress + Hauser Promass 80A Coriolis flow meter. Finally, a low-pressure filter, a purge/pressure regulator and an emergency shut-off valve followed the mass flow meter, before a flex hose connected the gas path to the injector block. The NG injector block was installed upstream of the intake surge tank to facilitate the mixing of the fuel with the boosted air. An injector driver controlled the pulse width of the gas injectors and allowed to run the engine under varying ratios of diesel and NG by changing the NG mass flow rate ( $\dot{m}_{NG}$ ).

A dedicated engine control unit (ECU) was used to control the high-pressure common rail diesel injection system, which supported up to three injections per cycle. Two Endress + Hauser Promass 83A Coriolis flow meters were used to determine the diesel mass flow rate ( $\dot{m}_{diesel}$ ) by measuring the total fuel supplied to and from the diesel high-pressure pump and injector.

### Fuel properties

During the dual-fuel operation, direct-injected diesel triggered the ignition of the bulk fuel mass of port fuel injected NG. The relevant properties of the diesel and

NG fuel used in this work are listed in Table 3. Three different gas compositions were purchased from Air Products to simulate typical NG mixtures available in the market:<sup>14</sup>

- Mix 1 has a high MN due to the relatively higher concentration of  $N_2$  and represents a part boil-off gas and part vaporised LNG fuel.
- Mix 2 works as a reference fuel due to the simplified composition, containing only  $CH_4$  and a small percentage of  $C_2H_6$ .
- Mix 3 represents an NG fuel with a relatively low MN, despite the high concentration of  $CH_4$ .

The NG surrogates listed above were carefully designed to evaluate the effects of MN on dual-fuel combustion characteristics, performance and emissions. The mole fraction of  $CH_4$  was held within a range of  $\pm 1.5\%$  to minimise an indirect effect on methane slip (e.g. engine-out  $CH_4$  emissions). The presence of  $C_2H_6$  and  $C_3H_8$  can shorten the ignition delay<sup>40,54,55</sup> and the burn rate,<sup>56</sup> while a higher mass fraction of  $N_2$  can slow down the reaction rates.<sup>37</sup>

The preferred method for calculating the MN was given by an online calculator developed by DNV GL for LNG.<sup>57</sup> According to Van Essen et al.,<sup>34</sup> this MN calculation uses the combustion properties of the fuel mixture and is based on a methane-propane scale referred to as Propane Knock Index (PKI). Nevertheless, the results of other MN algorithms demonstrated a similar trend for the three mixtures investigated in this study (see Table 3).

Another important parameter for the dual-fuel operation is the gas energy ratio (GER), which is given by the ratio of the energy content of the NG injected to the total fuel energy supplied to the engine. As revealed in Table 3, the use of a GER of 80% can reduce exhaust  $CO_2$  emissions by approximately 20% when assuming the complete conversion of hydrocarbon fuel into  $CO_2$  and that the brake efficiency of the dual-fuel engine is the same of the conventional diesel engine.

$$GER = \frac{\dot{m}_{NG} LHV_{NG}}{\dot{m}_{NG} LHV_{NG} + \dot{m}_{diesel} LHV_{diesel}}$$

### Exhaust emissions measurements and analysis

Exhaust emissions, such as  $CO$ ,  $CH_4$ ,  $NO_x$  and  $THC$ , were measured with a Horiba MEXA-7170 DEGR emissions analyser equipped with a heated line. The concentration of gaseous emissions in the exhaust stream was converted from parts per million (ppm) to net indicated specific emissions (in g/kWh). These were referred to ISCO, ISCH<sub>4</sub>, ISNO<sub>x</sub> and ISTHC, respectively, and were calculated using the methodology described in Regulation number 49 of the UN/ECE.<sup>10</sup> The aforementioned regulation also required the conversion of  $NO_x$  and  $CO$  emissions to a wet basis by applying a correction factor for the raw exhaust gas which is

**Table 3.** Fuel properties.

Property	Unit	Diesel	Natural gas (NG)		
			Mix 1	Mix 2	Mix 3
Methane number (MN)					
DNV GL (PKI) <sup>57</sup>	–	–	94.1	87.6	80.9
Wärtsilä <sup>58</sup>	–	–	96.0	89.0	82.0
MWM <sup>59</sup>	–	–	95.0	88.0	85.0
Cummins Westport <sup>60</sup>	–	–	89.2	85.9	82.4
Lower heating value ( $LHV_{fuel}$ )	MJ/kg	42.9	47.9	49.8	48.9
Wobbe index (WI)	MJ/Nm <sup>3</sup>	–	49.3	51.5	51.1
Stoichiometric air fuel ratio ( $AFR_{fuel}$ )	–	14.5	16.5	17.1	16.8
Gas density (101.325 kPa, 15°C)	kg/m <sup>3</sup>	–	0.700	0.708	0.725
Air Products material number	–	–	363815	359987	364241
Cetane number	–	> 45	–	–	–
Liquid density (101.325 kPa, 20°C)	kg/dm <sup>3</sup>	0.827	–	–	–
Gas composition (mole fraction)					
Methane (CH <sub>4</sub> )	%	–	96.4	95.0	94.0
Ethane (C <sub>2</sub> H <sub>6</sub> )	%	–	0.8	5.0	3.0
Propane (C <sub>3</sub> H <sub>8</sub> )	%	–	0.4	–	2.0
Nitrogen (N <sub>2</sub> )	%	–	2.4	–	1.0
Fuel contents (mass fraction)					
Carbon (%C <sub>fuel</sub> )	%	86.6	72.0	75.3	74.3
Hydrogen (%H <sub>fuel</sub> )	%	13.2	24.0	24.7	24.1
Nitrogen (%N <sub>fuel</sub> )	%	–	4.0	–	1.6
Oxygen (%O <sub>fuel</sub> )	%	0.2	–	–	–
Calculated carbon intensity					
Assuming the complete conversion of hydrocarbon fuel into CO <sub>2</sub>	gCO <sub>2</sub> /MJ	73.9	55.1	55.4	55.6
Maximum theoretical CO <sub>2</sub> reduction	%	–	25.5	25.1	24.7
considering a constant brake efficiency					
Estimated CO <sub>2</sub> reduction with a GER = 80%	%	–	20.4	20.1	19.8

dependent on the in-cylinder fuel mixture composition. The measurement of the THC was performed on a wet basis by a heated flame ionisation detector (FID). An AVL 415SE smoke metre was used to determine the concentration of black carbon containing soot, which was reported on a filter smoke number (FSN) basis.

### Data acquisition

The instantaneous in-cylinder pressure was measured by a Kistler 6125C piezoelectric pressure sensor coupled with an AVL FI Piezo charge amplifier. Intake and exhaust manifold pressures were measured by two Kistler 4049A water-cooled piezoresistive absolute pressure sensors coupled to Kistler 4622A amplifiers. Temperatures and pressures at relevant locations were measured by K-type thermocouples and pressure gauges, respectively. Two data acquisition (DAQ) cards and a personal computer were used to acquire the signals from the measurement devices. A USB-6251 high-speed DAQ card received the crank angle resolved data synchronised with an optical encoder of 0.25 CAD resolution. A USB-6210 low-speed DAQ card acquired the low-frequency engine operation conditions. These

data were displayed live by an in-house developed DAQ program and combustion analyser.

### Data analysis

Crank angle based in-cylinder pressure traces were averaged over 200 consecutive cycles for each operating point and used to calculate the IMEP and the apparent net heat release rate (HRR). Since the absolute value of the heat released is not as important to this study as the bulk shape of the curve to crank angle, a constant ratio of specific heats ( $\gamma$ ) of 1.33 was assumed throughout the engine cycle. The pressure rise rate (PRR) was represented by the average of the maximum pressure variations of 200 cycles of cylinder pressure versus crank angle. Combustion and in-cylinder flow stability were monitored by the coefficient of variation of IMEP (COV<sub>IMEP</sub>) over the sampled cycles.

The mass fraction burned (MFB) was given by the ratio of the integral of the HRR to the maximum cumulative heat release. Combustion phasing was determined by the crank angle of 50% (CA50) cumulative heat release. Combustion duration (CA10–CA90) was represented by the period between the crank angles of 10%

**Table 4.** Dual-fuel engine testing conditions.

Parameter	Unit	Low load	Medium load	High load
Engine load (IMEP)	MPa	0.6	1.2	1.8
Engine speed	rpm	1200	1200	1200
Diesel injection pressure	MPa	100	130	160
Gas energy ratio (GER)	%	80 ± 1	80 ± 1	80 ± 1
Test cell ambient air temperature	°C	30 ± 2	35 ± 3	40 ± 3
Intake manifold air temperature	°C	42 ± 1	43 ± 1	44 ± 1
Intake manifold air pressure	kPa	125	190	260
Exhaust manifold pressure	kPa	135	200	270
Exhaust gas recirculation (EGR)	%	0	0	0

(CA10) and 90% (CA90) cumulative heat release. The mean in-cylinder gas temperature at any crank angle position was computed by the ideal gas law.<sup>52</sup>

A current probe was used to acquire the electric current signal sent from the ECU to the diesel injector solenoid. The signal was corrected by adding the respective energising time delay, which was previously measured in a constant volume chamber. The resulting diesel injector current signal allowed for the determination of the actual start of diesel injection. In the case of multiple diesel injections, it was necessary to determine the split ratio between the first and second injections. This was given by the ratio of the energising time of each injection to the total energising time.

Ignition delay was defined as the period between the actual start of diesel injection and the start of combustion (SOC), set to 0.3% MFB point of the averaged cycle. After the calculation of the combustion characteristics (e.g. CA50) and ignition delay, the average in-cylinder pressure and the resulting HRR were smoothed using a Savitzky-Golay filter.

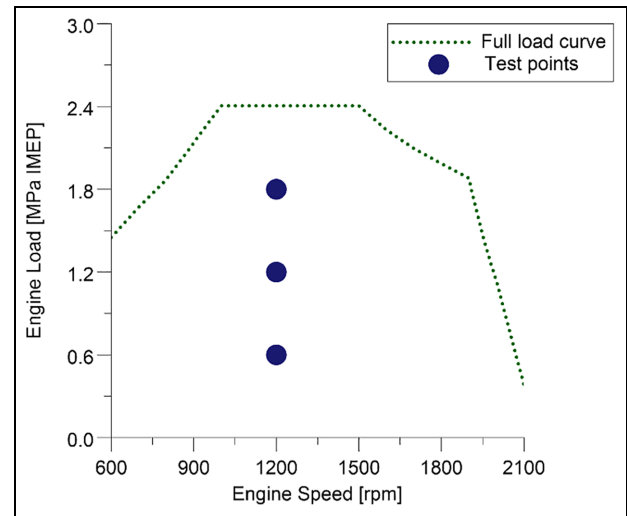
The ratio of the work done to the rate of fuel energy supplied to the engine was represented by the net indicated efficiency as

$$\begin{aligned} \text{Net indicated efficiency} \\ = \frac{3.6P_{ind}}{(\dot{m}_{diesel}LHV_{diesel}) + (\dot{m}_{NG}LHV_{NG})} \end{aligned}$$

where  $P_{ind}$  is the engine net indicated power calculated from the measured IMEP. Combustion efficiency calculations were based on the emissions products not fully oxidised during the combustion process except soot as

$$\begin{aligned} \text{Combustion efficiency} \\ = \left\{ 1 - \frac{P_{ind}}{10^3} \left[ \frac{(ISCO LHV_{CO}) + (ISHC LHV_{NG})}{(\dot{m}_{diesel}LHV_{diesel}) + (\dot{m}_{NG}LHV_{NG})} \right] \right\} \end{aligned}$$

where  $LHV_{CO}$  is equivalent to 10.1 MJ/kg.<sup>52</sup> Combustion losses associated with THC emissions were hypothesised to be a result of unburned NG fuel only. This can be considered a conservative approach as the  $LHV_{NG}$  for the three NG compositions used in this study are higher than the  $LHV_{diesel}$ .

**Figure 3.** Experimental test points over an estimated HD engine speed-load map.

Finally, the lambda was calculated as

$$\text{Lambda} = \frac{\dot{m}_{air}}{\dot{m}_{NG}AFR_{NG} + \dot{m}_{diesel}AFR_{diesel}}$$

## Test methodology

Dual-fuel engine testing with three different NG compositions was carried out under steady-state loads of 0.6, 1.2 and 1.8 MPa IMEP and an engine speed of 1200 rpm. These loads are equivalent to 25%, 50% and 75% of full engine load, respectively, and represent high residency areas in a typical HD vehicle drive cycle such as the WHSC. The location of these test points over an estimated speed and load map can be seen in Figure 3. Stable engine operation was quantified by COV<sub>IMEP</sub> values of less than 5%.

The test conditions are summarised in Table 4. The GER was held at 80% ± 1%, regardless of the NG mixture. The high substitution ratio was selected in order to maximise the use of NG and help to achieve a GER<sub>WHTC</sub> of more than 68%. The intake and exhaust manifold pressure setpoints were taken from a Euro V



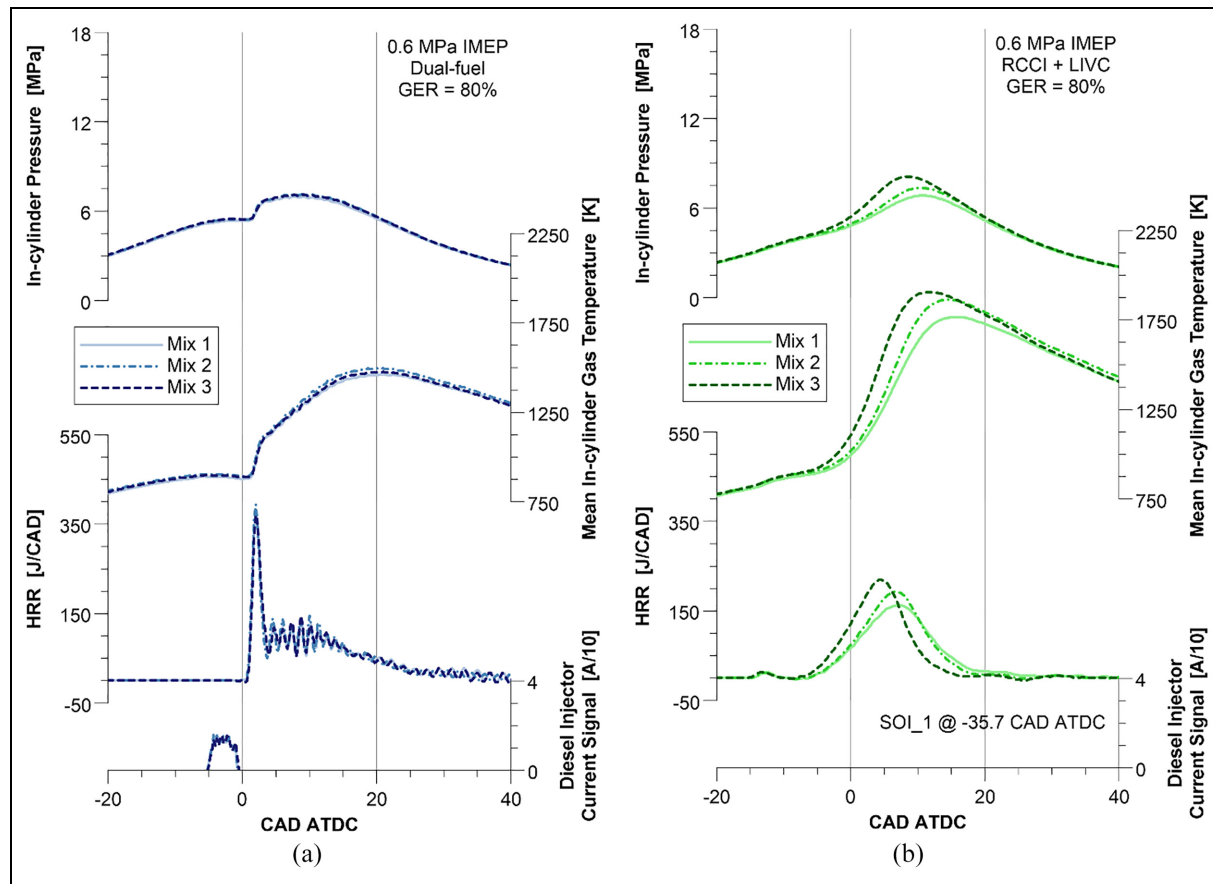


**Figure 4.** The effects of NG composition on: (a) conventional dual-fuel and (b) RCCI combustion modes at a low engine load of 0.6 MPa IMEP.

**Table 5.** ECR and optimum diesel injection strategies for the conventional dual-fuel and RCCI combustion modes investigated in this study.

Combustion mode	ECR	Low load	Medium load	High load
Dual-fuel	16.8	Late single, SOI_1 @ -5.2 CAD ATDC	Late single, SOI_1 @ -1.0 CAD ATDC	Late single, SOI_1 @ 5.0 CAD ATDC
RCCI + LIVC	13.8	Early single, SOI_1 @ -35.7 CAD ATDC	Late split, SOI_1 @ -60 CAD ATDC, SOI_2 @ 6.2 CAD ATDC, split ratio of 49/51	Late split, SOI_1 @ -60 CAD ATDC, SOI_2 @ 8.5 CAD ATDC, split ratio of 41/59

compliant multi-cylinder HD diesel engine in order to provide a sensible starting point. This was necessary because an external boosting device and a back-pressure valve were used in place of a turbocharger.

The study was performed without external exhaust gas recirculation (EGR) in order to simplify the experimental investigation. Nevertheless, all comparisons were carried out for the cases that attained the highest net indicated efficiency and/or an engine-out NO<sub>x</sub> of less than 8.5 g/kWh. This imposed trade-off was necessary in order to simulate a Euro VI emissions compliance with a NO<sub>x</sub> conversion efficiency of approximately 95% in the selective catalyst reduction (SCR) system.

Moreover, conventional dual-fuel engine operation at the baseline ECR of 16.8 was compared against an RCCI combustion at a lower ECR of 13.8. The RCCI operation was combined with a LIVC strategy in order to adjust the in-cylinder lambda and the charge reactivity, targeting higher levels of combustion efficiency and exhaust gas temperature (EGT). The ECR of 13.8 represented the latest LIVC that could be used without adversely affecting the combustion stability and soot emissions.

The selected diesel injection strategies are depicted in Table 5. The conventional dual-fuel operation was achieved with a single diesel injection near TDC at all engine loads. The RCCI combustion, however,



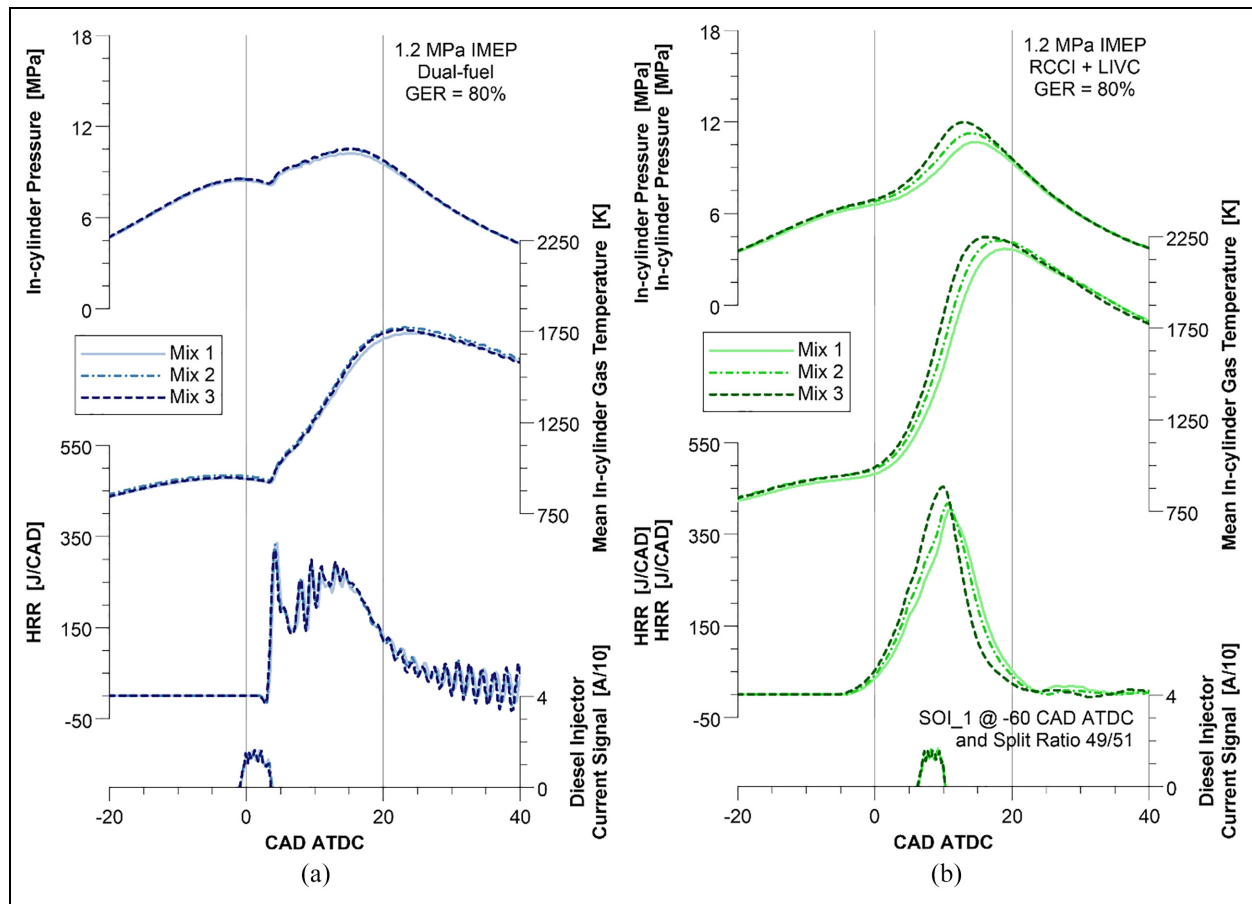


**Figure 5.** The effects of NG composition on: (a) conventional dual-fuel and (b) RCCI combustion modes at a medium engine load of 1.2 MPa IMEP.

employed an early single diesel injection at low load and a late split injection strategy at medium and high engine loads. In the case of a late split injection strategy, the diesel fuel energy supplied to the engine during the first injection had to be reduced as the engine load was increased. This was necessary to control the combustion process within the upper bounds for calibration, which were linked to engine hardware limitations and consisted primarily of a PRR limit of 2.0 MPa/CAD and a maximum average in-cylinder pressure (P<sub>MAX</sub>) of 18 MPa. The start of the first diesel injection (SOI<sub>1</sub>) was held constant at −60 CAD ATDC while the second diesel injection (SOI<sub>2</sub>) and the average split ratio were swept.

The optimum engine calibrations were attained after a long optimisation process with Mix 2, which targeted the previously described trade-off between NO<sub>x</sub> emissions and net indicated efficiency. The use of earlier diesel injection timings generally increased NO<sub>x</sub> emissions with minimal improvement in net indicated efficiency. The only exception to this trend was for the RCCI regime at the lowest engine load of 0.6 MPa IMEP. At this condition, a more advanced SOI<sub>1</sub> actually reduced both NO<sub>x</sub> emissions and net indicated efficiency via a more homogenous and later combustion

event.<sup>21</sup> Finally, the diesel injection strategies were not modified when testing the dual-fuel engine with the other two NG compositions. This approach simplified the experimental analysis and allowed to highlight any weakness a dual-fuel engine calibration might have when experiencing a change in the NG quality.

## Results and discussion

### Combustion analysis

The effects of NG composition on conventional dual-fuel and RCCI engine modes with a constant GER of approximately 80% are depicted in Figures 4–6. The combustion characteristics of the conventional dual-fuel mode remained nearly identical when changing the NG fuel mixture at a given engine load, suggesting that MN has little impact on the HRR of the dual-fuel combustion with a single diesel injection near TDC. This finding can be attributed to the fact that the ignition and burning of the bulk mass of NG were highly dependent on the high-temperature turbulent diffusion flames created by the diesel fuel. At such conditions, the premixed gas temperature did not reach its autoignition temperature and the mixture reactivity relied mostly

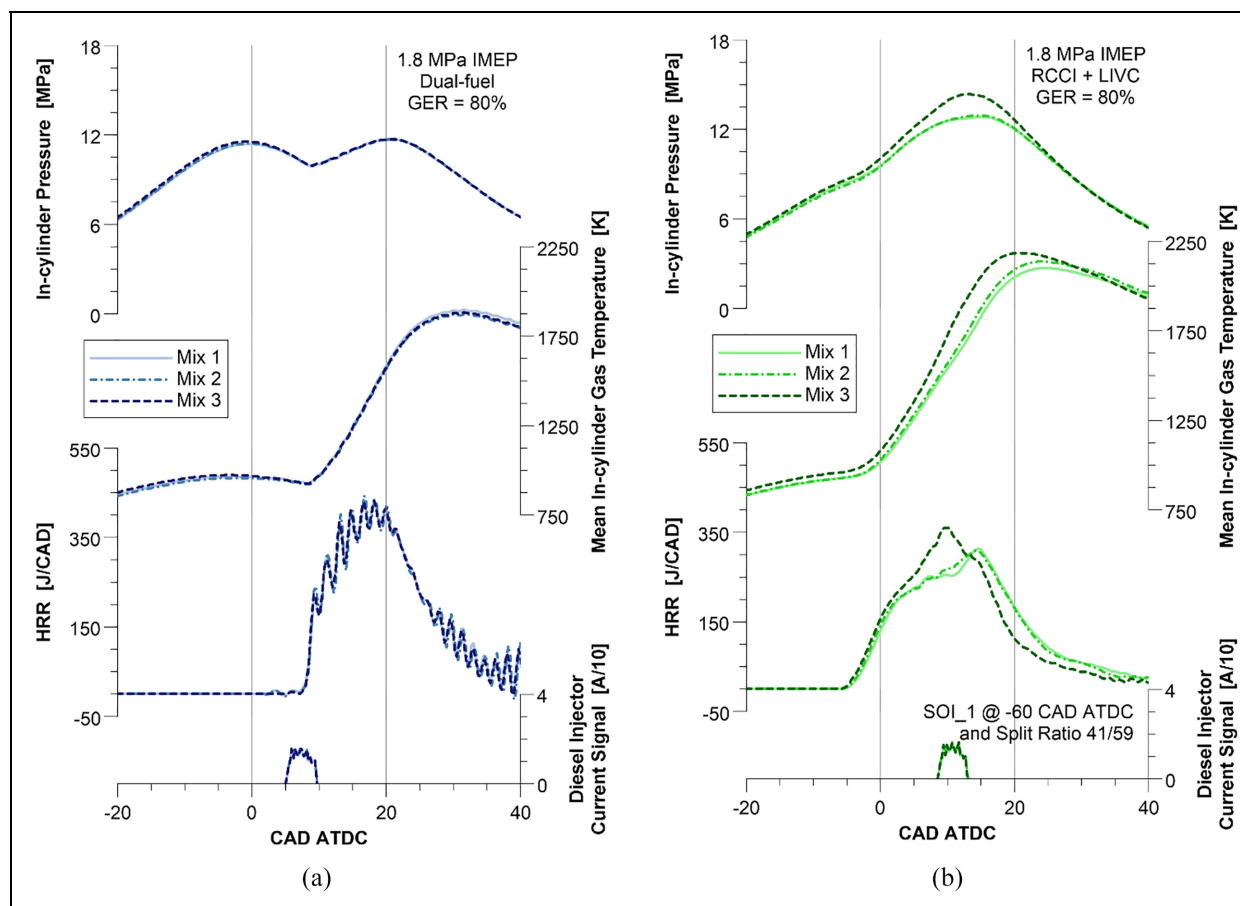


**Figure 6.** The effects of NG composition on: (a) conventional dual-fuel and (b) RCCI combustion modes at a high engine load of 1.8 MPa IMEP.

upon the local oxygen concentration rather than on the NG properties.<sup>55</sup>

Moreover, there was a reduction in the first peak heat release of the conventional dual-fuel combustion when increasing the engine load from 0.6 to 1.8 MPa IMEP. This behaviour was associated with a shorter ignition delay measured at elevated engine loads (see Figure 7), which was induced by the increased charge reactivity (e.g. fuel-rich mixtures) and the higher in-cylinder gas pressures and temperatures at such conditions.<sup>31,55</sup> The aforementioned effect can be demonstrated by the ignition delay of  $-1.75$  CAD recorded at 1.8 MPa, where all three NG mixtures had the onset of the low-temperature heat release (LTHR) prior to the diesel injection at a calculated in-cylinder gas temperature of approximately  $950^{\circ}\text{C}$ .

The RCCI mode, however, was more sensitive to changes in the NG composition. This was demonstrated by the larger variations in P<sub>MAX</sub> and peak HRR, particularly when using an early single diesel injection at 0.6 MPa IMEP. The higher sensitivity to the NG fuel properties was attributed to the fact that RCCI

combustion is dependent upon the autoignition characteristics of the in-cylinder charge. Diesel fuel supplied to the engine during the SOI<sub>1</sub> increased the reactivity of the in-cylinder mixture and created favourable conditions for the compression ignition of NG. Consequently, NG fuels with a higher concentration of  $\text{C}_3\text{H}_8$  and thus a lower MN were faster to ignite, as demonstrated by the more advanced SOC for the RCCI mode with Mix 3 in Figure 7.

Nevertheless, RCCI combustion presented significantly longer ignition delays between the SOI<sub>1</sub> and SOC than the conventional dual-fuel mode. This was primarily due to the use of early SOI<sub>1</sub>s targeting the colder squish zone. The lower compression temperatures obtained via a LIVC strategy also helped to slow down the reaction rates and maintain a sufficiently long ignition delay despite the relatively richer mixtures at a given engine load. Nevertheless, the increase in charge reactivity and the formation of multiple compression ignition sites via early diesel injections yielded more advanced SOC in the RCCI mode. As a result, the second diesel injection used at 1.2 and 1.8 MPa IMEP took

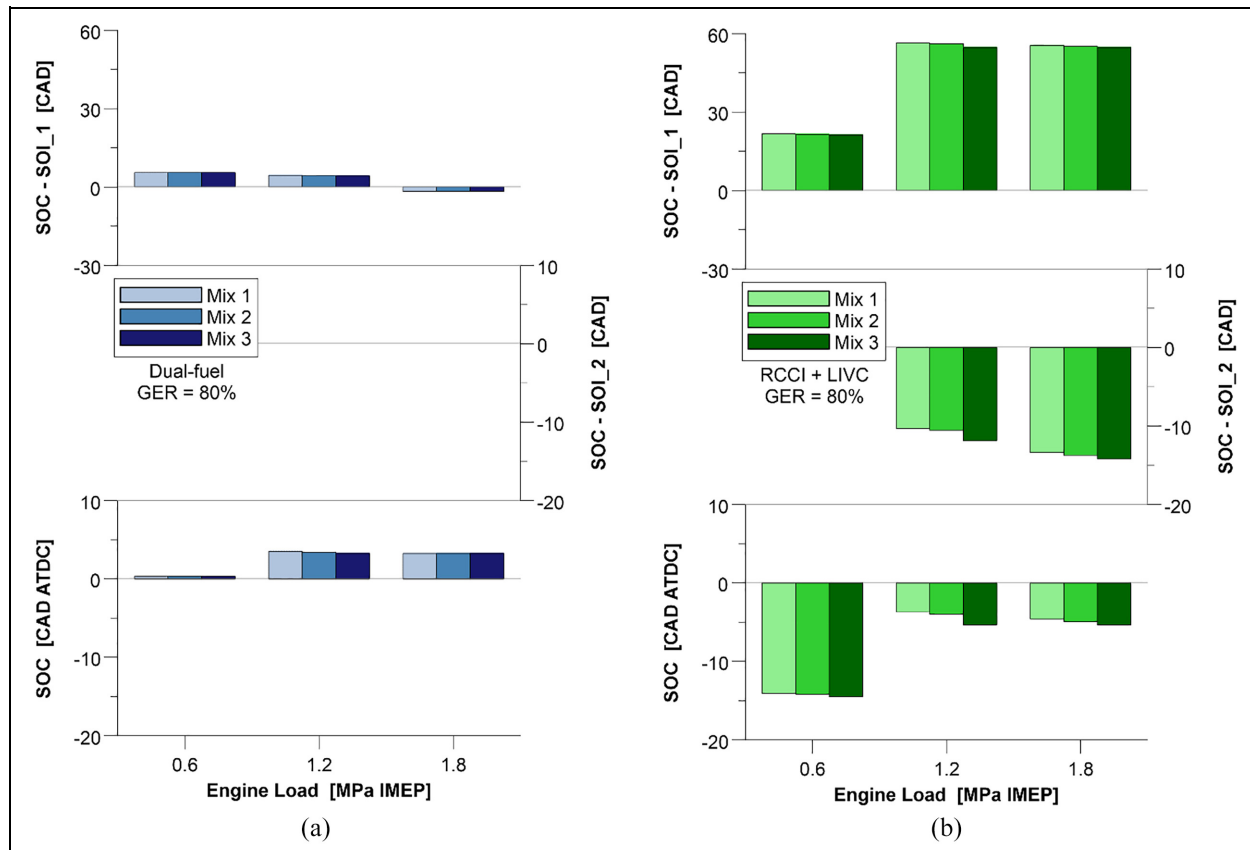


**Figure 7.** The effects of NG composition on the start of combustion (SOC) and ignition delay (e.g. time between start of diesel injections and SOC) of: (a) conventional dual-fuel and (b) RCCI combustion modes.

place after the combustion had already started, as supported by the negative ignition delays between SOI<sub>2</sub> and SOC in Figure 7.

To avoid excessive PRR and control the levels of P<sub>MAX</sub>, the amount of diesel fuel injected during the SOI<sub>1</sub> had to be reduced as the engine load was increased from 0.6 to 1.8 MPa IMEP (see Table 5). This was due to the shorter ignition delays observed at higher engine loads, following the same trend of the conventional dual-fuel combustion. Finally, extra attention is required when switching from the conventional dual-fuel to the RCCI mode, particularly when operating the engine with low MN fuels. The NG injector pulse width (e.g. mass flow rate) and the resulting GER must be reduced before adding diesel fuel via an early single or through the first injection event of the late split diesel injection strategy.

The effects of engine load and NG composition on additional combustion characteristics are depicted in Figures 8 and 9. The increase in engine load from 0.6 to 1.8 MPa IMEP required a delay in the CA<sub>50</sub> to maintain both dual-fuel operating modes within the upper limits of P<sub>MAX</sub>, PRR and NO<sub>x</sub> emissions. This combustion control was achieved through a later SOI<sub>1</sub> in the conventional dual-fuel regime and by injecting less

diesel fuel at the SOI<sub>1</sub> or retarding SOI<sub>2</sub> in the RCCI mode.

In general, the RCCI operation with LIVC allowed for more advanced CA<sub>50</sub> and CA<sub>90</sub> positions than the conventional dual-fuel cases. This was likely a result of lower local combustion temperatures, which allowed for earlier optimum combustion processes. Moreover, combustion duration was typically shorter in the RCCI regime except at the highest load of 1.8 MPa IMEP, where slightly earlier CA<sub>90</sub>s did not compensate for the more advanced SOC and increased the CA<sub>10</sub>–CA<sub>90</sub> period. Nevertheless, a more homogenous and progressive combustion process, induced by the reactivity of the diesel fuel injected during the first injection, yielded lower levels of PRR and COV<sub>IMEP</sub> than the conventional dual-fuel mode with a late single diesel injection. These benefits were often achieved at the expense of higher P<sub>MAX</sub> levels.

In terms of NG quality, changes in the fuel composition had little impact on the HRR characteristics of the conventional dual-fuel regime. However, the use of NG fuels with a lower MN such as Mix 3 shortened the CA<sub>10</sub>–CA<sub>90</sub> period of the RCCI regime at all engine loads. This resulted in relatively more advanced CA<sub>50</sub> and CA<sub>90</sub> positions as well as higher levels of PRR and

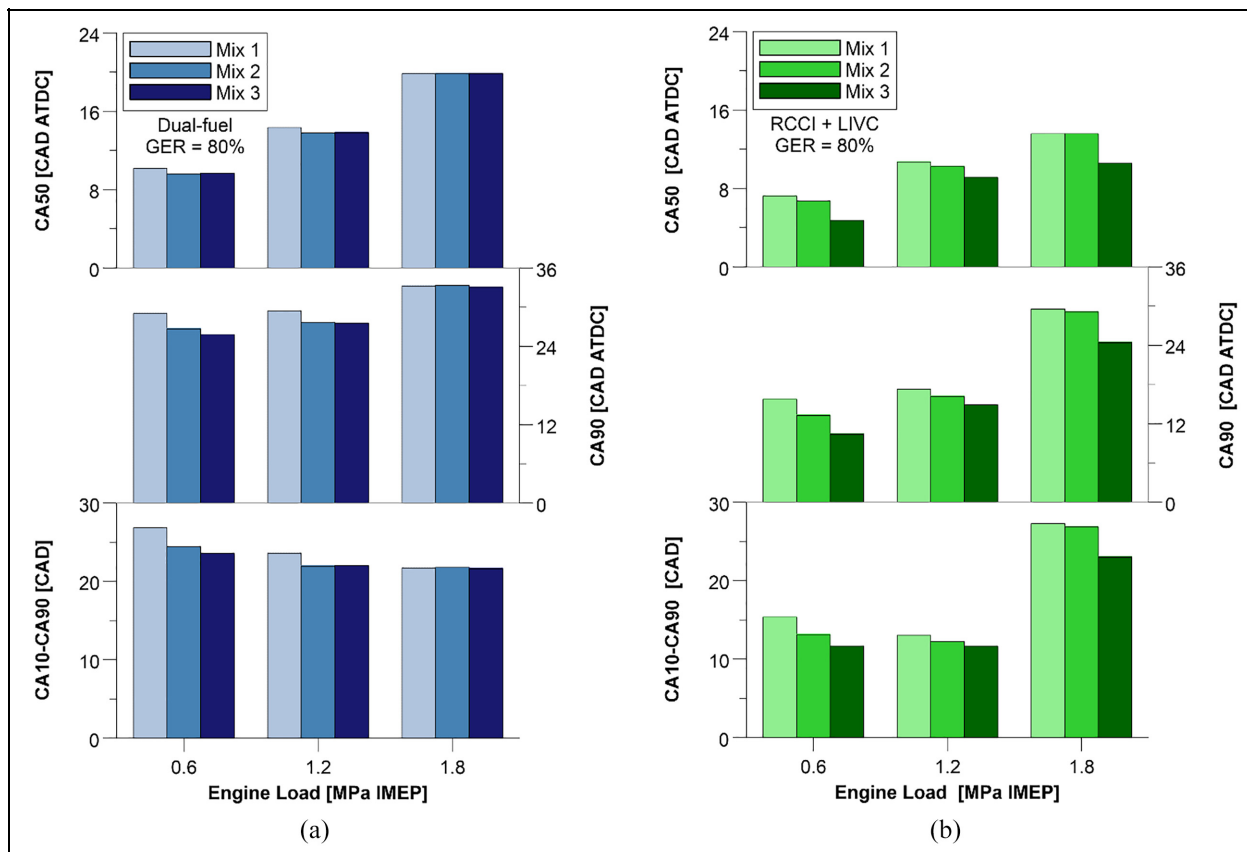


**Figure 8.** The effects of NG composition on the HRR characteristics of: (a) conventional dual-fuel and (b) RCCI combustion modes.

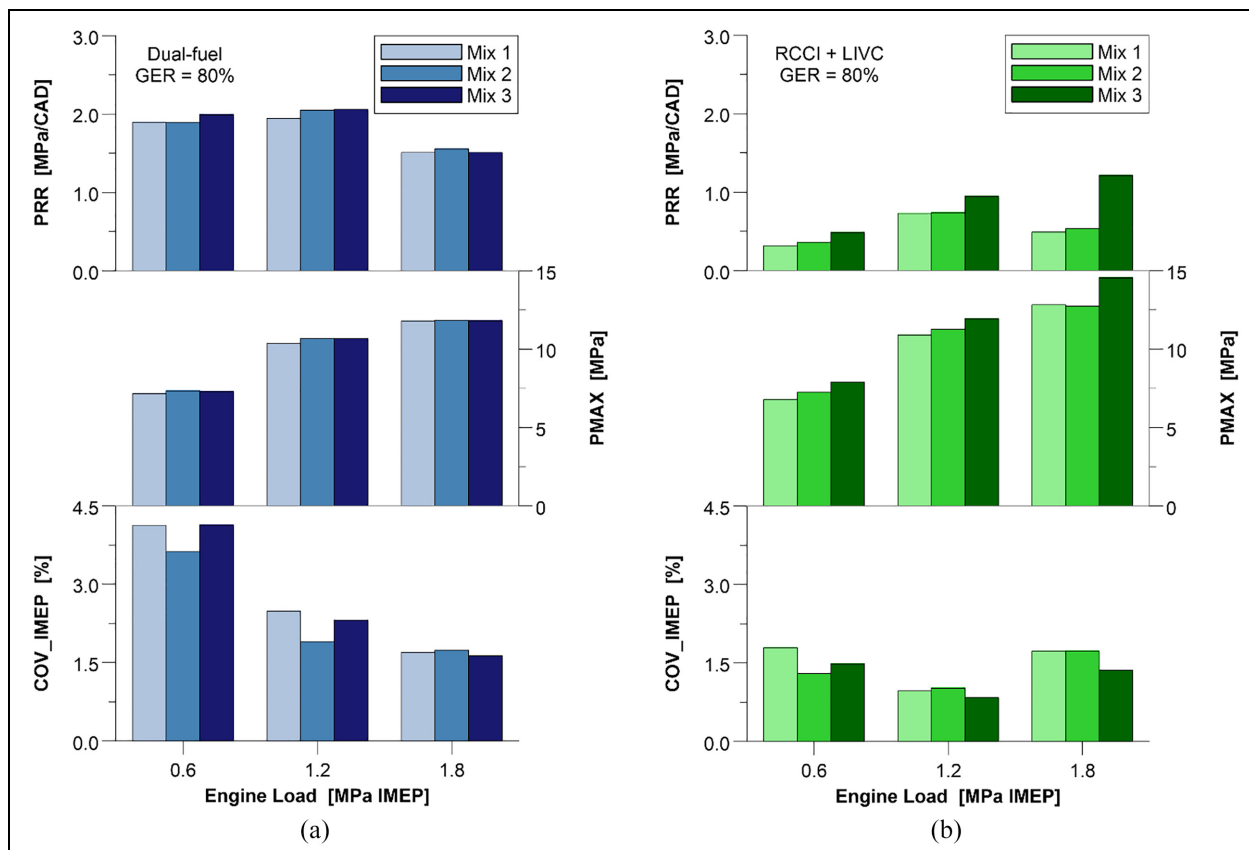


**Figure 9.** The effects of NG composition on additional combustion characteristics of: (a) conventional dual-fuel and (b) RCCI combustion modes.

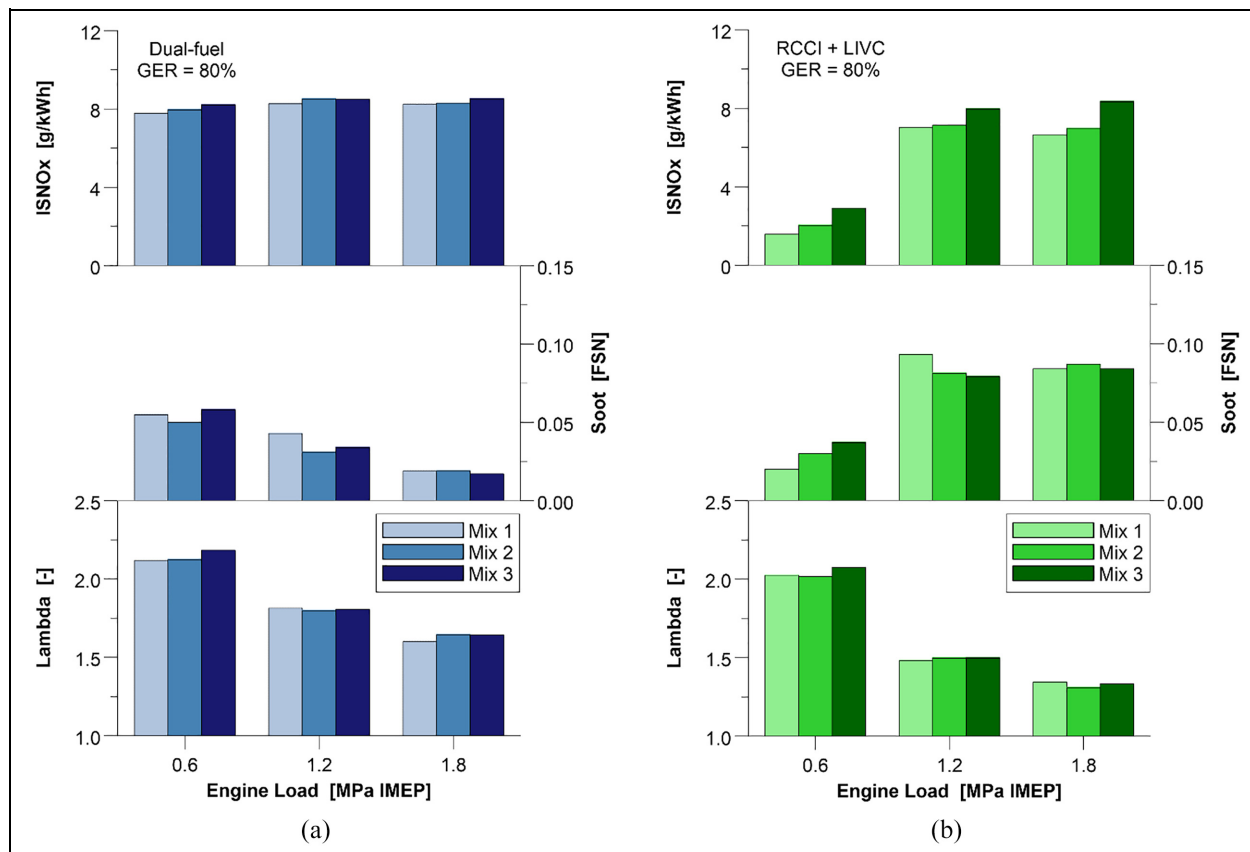


**Figure 10.** The effects of NG composition on NOx emissions, soot and lambda of: (a) conventional dual-fuel and (b) RCCI combustion modes.

PMAX. As mentioned earlier, this sensitivity to the NG composition was associated with the presence of more reactive fuel components (e.g.  $C_2H_6$  and  $C_3H_8$ ) that potentially helped to shorten the ignition delay,<sup>40,54</sup> increase local flame speed<sup>61,62</sup> and create favourable conditions for the autoignition of the bulk NG fuel.<sup>19</sup>

The most significant differences in HRR characteristics caused by the NG fuel properties occurred under an RCCI operation at 0.6 and 1.8 MPa IMEP. The sensitivity of parameters like CA50, CA90 and PRR to the NG composition was attributed to the presence of a relatively higher quantity of diesel fuel at the SOI<sub>1</sub> at 0.6 MPa IMEP (e.g. theoretical split ratio of 100/0) and due to the lower lambda and higher in-cylinder charge reactivity experienced by the RCCI regime at 1.8 MPa IMEP.

### Engine-out emissions

Engine-out emissions for dual-fuel operations with different NG compositions are depicted in Figures 10 and 11. The use of a low MN gas such as Mix 3 increased NOx emissions, particularly when running the engine in the more sensitive RCCI mode. The lower resistance to autoignition probably increased local combustion

temperatures when compared to those obtained with a high MN fuel (e.g. Mix 1). Soot levels were maintained below 0.1 FSN for all cases as the diesel fuel represented only 20% of the total energy supplied to the engine.

Additionally, NG composition had little impact on soot emissions at a given engine load and dual-fuel regime. This was likely due to a trade-off between local temperatures and mixture formation, where the hotter dual-fuel combustion with a low MN fuel compensated for the slightly worse fuel-air mixing process induced by the shorter ignition delay. The only exception occurred for an RCCI operation at 0.6 MPa IMEP, where NOx and soot increased simultaneously as the MN was reduced. This was attributed to the relatively early CA90s and lower late-cycle gas temperatures attained with Mix 2 and 3, which offset the increase in local combustion temperatures and deteriorated the soot oxidation process. Lambda was relatively insensitive to changes in MN, and small differences were likely associated with variations in  $LHV_{fuel}$ ,  $AFR_{fuel}$  and net indicated efficiency.

Conventional dual-fuel combustion was NOx limited at all engine loads. This required adjustments in the SOI<sub>1</sub> as the engine load was increased in order to

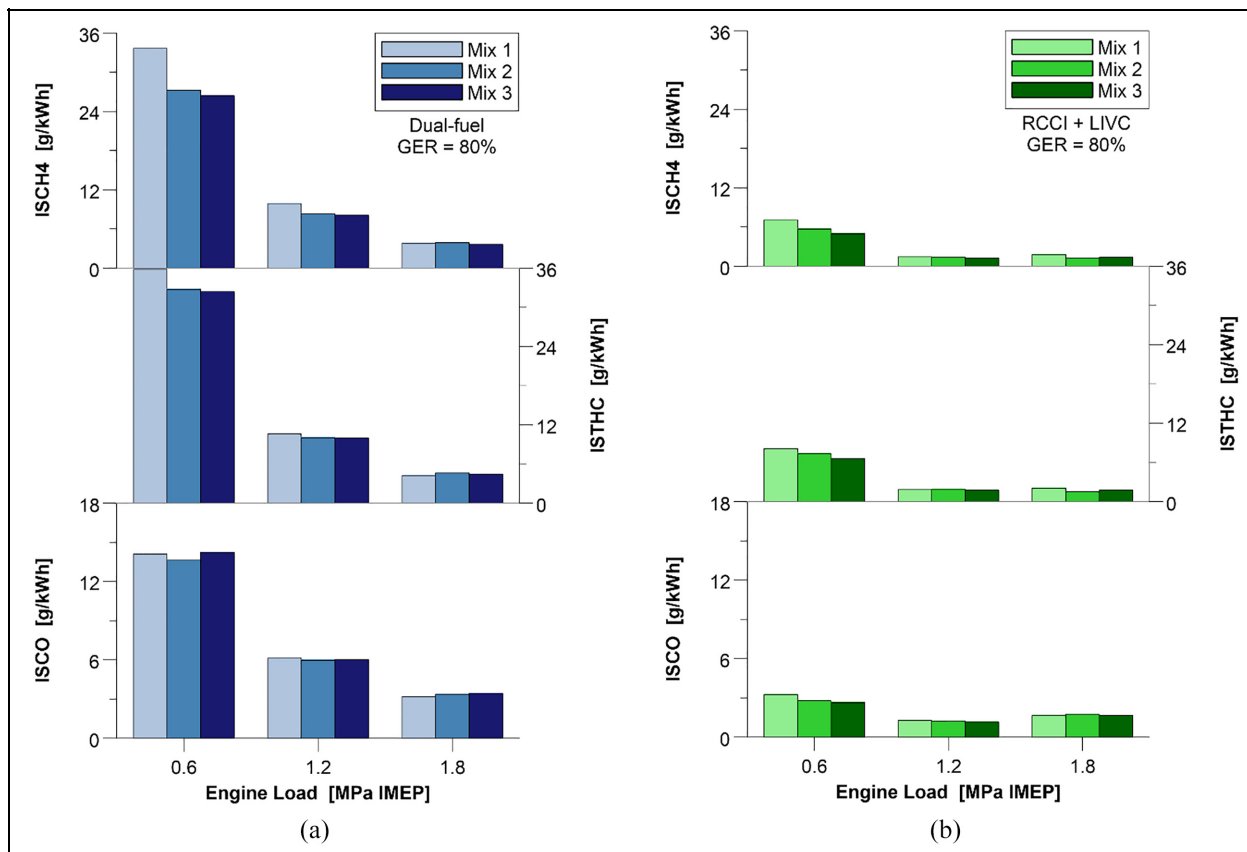


**Figure 11.** The effects of NG composition on CH<sub>4</sub>, THC and CO emissions of: (a) conventional dual-fuel and (b) RCCI combustion modes.

reduce peak combustion temperatures and maintain the levels of NO<sub>x</sub> within the target of less than 8.5 g/kWh. Alternatively, the RCCI operation with LIVC decreased NO<sub>x</sub> emissions by up to 80% (to a minimum of 1.6 g/kWh at 0.6 MPa IMEP) when compared to the conventional dual-fuel mode. The reduction in engine-out NO<sub>x</sub> emissions did not correlate well with the increase in the calculated peak mean in-cylinder gas temperature shown in Figures 4 to 6. The relatively lower levels of NO<sub>x</sub> were associated with the formation of a more homogeneous fuel-air mixture and lower local combustion temperatures.<sup>5</sup> Moreover, the use of LIVC in the RCCI mode potentially helped reduce NO<sub>x</sub> emissions by lowering the lambda and thus the oxygen availability.

The increase in engine load to 1.2 and 1.8 MPa IMEP, however, minimised the NO<sub>x</sub> reduction benefit of the RCCI combustion. This was due to a decrease in the amount of diesel fuel at SOI<sub>1</sub> (e.g. lower split ratio), which led to a more diffusive dual-fuel combustion process.<sup>15</sup> Consequently, the presence of locally fuel-rich zones created by the second diesel injection elevated the levels of soot at mid- and high load RCCI operations. The use of an early diesel injection at 0.6 MPa IMEP allowed for lower soot emissions than the conventional dual-fuel combustion.

Nevertheless, the RCCI mode with LIVC achieved the lowest levels of CH<sub>4</sub>, THC and CO emissions, as shown in Figure 11. This improvement over the

conventional dual-fuel combustion was attained at all engine loads and was primarily a result of an increased in-cylinder charge reactivity promoted by the diesel fuel injected earlier in the cycle. On average, the relative reductions in ISCH<sub>4</sub>, ISCHC and ISCO achieved approximately 81% at 0.6 and 1.2 MPa IMEP and about 57% at 1.8 MPa IMEP. The lowest levels of CH<sub>4</sub> emissions of 1.2–1.3 g/kWh were achieved by the RCCI regime with Mix 2 and 3 at the engine loads of 1.2 and 1.8 MPa IMEP. The decrease in lambda brought about by the use of LIVC also helped to increase the flammability of the in-cylinder charge when compared to a conventional dual-fuel operation at the baseline ECR. However, the excessively lean fuel-air mixtures and the low-temperature combustion limited the reduction in methane slip to 5.0–7.1 g/kWh at 0.6 MPa IMEP depending on the NG composition.

Dual-fuel engine operations with a low MN fuel (e.g. Mix 3) reduced the ISCH<sub>4</sub> and ISTHC in the majority of the test cases. This was attributed to higher local combustion temperatures, as supported by the increase in NO<sub>x</sub> emissions (see Figure 10). This effect was likely associated with the greater concentrations of C<sub>2</sub>H<sub>6</sub> and C<sub>3</sub>H<sub>8</sub> in the NG composition, which advanced the SOC and accelerated the dual-fuel combustion process. A similar trend had been reported in the literature when adding larger concentrations of ethane (e.g. 10% and 20%) into a



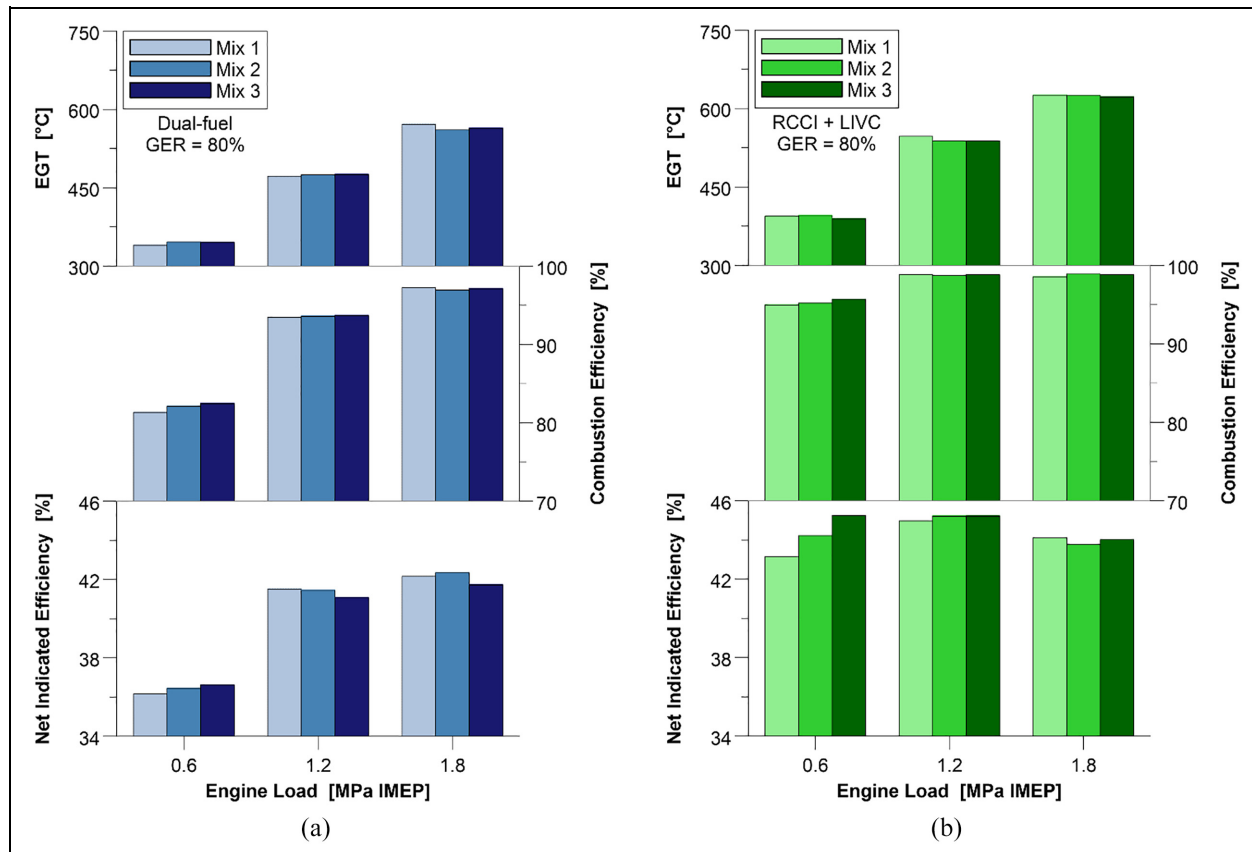


**Figure 12.** The effects of NG composition on EGT and efficiencies of: (a) conventional dual-fuel and (b) RCCI combustion modes.

gaseous mixture used in a conventional dual-fuel engine.<sup>19</sup> The reduction in MN, however, demonstrated little effect on ISCO. This indicates that the CO oxidation process could be controlled by the high reactivity and high-temperature zones created by the diesel injections rather than by the NG composition. Finally, the increase in engine load minimised CH<sub>4</sub>, THC and CO emissions regardless of the dual-fuel regime because of the relatively lower in-cylinder lambda and higher combustion temperatures.

### Engine performance

The effects of NG composition on exhaust gas temperature (EGT) and efficiencies at different loads are depicted in Figure 12. The alteration of the MN had little impact on the EGT of the conventional dual-fuel and RCCI operating modes. The differences of  $\pm 6^\circ\text{C}$  were most likely a result of changes in CA<sub>90</sub> position and day-to-day variations in the test cell ambient air temperature (see Table 4). However, the EGT was increased as more fuel was injected at higher engine loads, demonstrating the opposite trend of the lambda showed in Figure 10.

At 0.6 MPa IMEP, a reduction in MN increased the combustion efficiency and helped to improve upon the net indicated efficiency of both dual-fuel combustion

modes. This was attributed to the higher degree of premixed combustion experienced by both dual-fuel strategies at low engine loads, where a low MN fuel was able to aid the reactivity of the in-cylinder charge. Relatively earlier and shorter dual-fuel combustion processes with Mix 3 (see Figure 8) also brought the thermodynamic advantage of releasing the thermal energy closer to TDC and thus increasing the extraction of work during the expansion stroke.<sup>63</sup> The highest increase in net indicated efficiency of 4.9% (from 43.1% to 45.2%) was attained when switching the NG composition from Mix 1 to Mix 3 under an RCCI operation with LIVC.

There were, however, minimum improvements in combustion efficiency when using a low MN fuel at 1.2 and 1.8 MPa IMEP. At these particular loads, reductions in THC and CO emissions were probably offset by the differences in  $LHV_{fuel}$ , levelling out the combustion efficiency for the three NG compositions in both dual-fuel modes. Moreover, the use of Mix 3 decreased the net indicated efficiency when operating the engine in the conventional dual-fuel mode. This effect was likely a result of an increase in heat transfer losses introduced by the relatively higher combustion temperatures of the low MN fuel. In the RCCI regime, however, shorter and more advanced combustion with Mix 3 helped to maximise the expansion work and maintain similar levels of net indicated efficiency to



those achieved with the other NG fuels at mid- and high load conditions.

When comparing the two dual-fuel modes, RCCI operation with LIVC achieved an EGT in the order of 44–75°C higher than that measured for the conventional dual-fuel combustion with the baseline IVC. This was associated with a reduction in the intake mass flow rate via a lower ECR of 13.8, as supported by the reduction in  $\lambda$  (see Figure 10). The RCCI mode also attained an EGT of 390°C, on average, at 0.6 MPa IMEP. This level of temperature is beneficial for the methane oxidation catalyst (MOC) used in dual-fuel engines, as the device generally requires an EGT of more than 400°C for high CH<sub>4</sub> conversion efficiency.<sup>13,64</sup> The combination of this advanced dual-fuel strategy with cylinder deactivation<sup>65</sup> has the potential to achieve even higher EGTs and further improve upon the CH<sub>4</sub> conversion efficiency in MOCs.

Moreover, the RCCI mode with LIVC resulted in higher combustion efficiencies (of up to 98.9%) than a conventional dual-fuel operation (of up to 97.2%). The largest improvement was observed at a low engine load of 0.6 MPa IMEP, where the average combustion efficiency was increased from 82.0% in a conventional dual-fuel mode to 95.2% in the RCCI regime. This was attributed to reductions in the levels of CO, CH<sub>4</sub> and unburned HC emissions, as discussed in the previous Subsection.

Finally, the RCCI operation increased the net indicated efficiency at all engine loads when compared to the conventional dual-fuel mode. The highest relative increase was attained at 0.6 MPa IMEP, where the RCCI combustion with Mix 3 achieved a net indicated efficiency 45.2% – significantly higher than the 36.6% for a conventional dual-fuel mode with the same NG fuel. A net indicated efficiency of 45.2% was also obtained by the RCCI combustion with Mix 2 and Mix 3 at 1.2 MPa IMEP. The relatively low  $\lambda$  of 1.33, on average, limited the net indicated efficiency of the RCCI mode to approximately 44.0% at 1.8 MPa IMEP. An increase in  $\lambda$  via a higher boost pressure can potentially reduce heat transfer losses and increase the net indicated efficiency at such condition. However, further investigation is necessary to determine if the upper bounds for calibration (e.g. PMAX of 18 MPa) would limit the amount of diesel fuel injected at –60 CAD ATDC.

## Conclusion

In this study, engine experiments were performed to investigate the effects of natural gas (NG) composition on conventional dual-fuel and RCCI combustion modes. Testing was carried out with three gas mixtures of different methane numbers (MN) in a heavy-duty compression ignition engine equipped with a stock diesel piston, a high-pressure common rail diesel injection

system and a variable valve actuation system on the intake valves. The analysis was conducted without exhaust gas recirculation at a constant engine speed of 1200 rpm and three engine loads of 0.6, 1.2 and 1.8 MPa IMEP. The gas energy ratio (GER) was held at  $80\% \pm 1\%$  while the diesel injection strategy was optimised for the best trade-off between NO<sub>x</sub> emissions, PMAX, PRR and net indicated efficiency in both dual-fuel combustion modes. Miller cycle via late intake valve closing (LIVC) was used to decrease the effective compression ratio (ECR) and help control charge reactivity in the RCCI mode. The primary findings can be summarised as follows:

1. The RCCI combustion was more sensitive to changes in MN than the conventional dual-fuel operation. This was due to the fact the RCCI mode is reliant upon the autoignition characteristics of the in-cylinder charge, which were affected by the NG composition. Alternatively, conventional dual-fuel operation relied mostly on the high-temperature turbulent diffusion flames created by a late single diesel injection. Nevertheless, the optimum diesel injection timings remained the same for the three NG fuel mixtures at a given dual-fuel combustion mode. However, engine-out emissions and performance varied slightly.
2. A reduction in MN (from 94.1 to 80.9) advanced the combustion phasing and shortened the combustion duration in the majority of the test cases, resulting in higher combustion temperatures. This helped to minimise the THC and CH<sub>4</sub> emissions at the expense of higher NO<sub>x</sub> emissions, particularly when operating the engine in the RCCI combustion mode. Exhaust gas temperatures (EGT) were not significantly affected by NG composition, varying by  $\pm 6^\circ\text{C}$ .
3. In terms of performance, the most significant effects introduced by changes in the NG composition were observed on an RCCI operation at 0.6 MPa IMEP. At such a light load condition, the use of a low MN fuel helped to advance and accelerate the burn rate and to increase the combustion efficiency, resulting in 4.9% higher net indicated efficiency than the test case with a high MN fuel (45.2% vs 43.1%).
4. The RCCI operation with LIVC was shown as an effective means of simultaneously achieving lower NO<sub>x</sub> and CH<sub>4</sub> emissions than a conventional dual-fuel mode, particularly at low and medium engine loads. The lowest levels of NO<sub>x</sub> emissions (1.6–2.9 g/kWh) were attained with relatively low CH<sub>4</sub> emissions (5.0–7.1 g/kWh) at 0.6 MPa IMEP. The lowest levels of CH<sub>4</sub> emissions (1.2–1.4 g/kWh) were obtained with controlled NO<sub>x</sub> emissions (7.0–8.0 g/kWh) at 1.2 MPa IMEP. This improvement over the conventional dual-fuel mode was

accomplished at the expense of a more complex combustion control via multiple diesel injections and LIVC. Moreover, the second diesel injection used at 1.2 and 1.8 MPa IMEP contributed to slightly higher soot levels in the RCCI mode.

5. This study also revealed that the RCCI combustion with LIVC (ECR of 13.8) can increase the EGT by up to 75°C when compared to the conventional dual-fuel operation at the baseline ECR of 16.8. This characteristic will likely help to achieve higher levels of CH<sub>4</sub> conversion efficiency in the exhaust aftertreatment system, decreasing the amount of methane slip.

Overall, this experimental investigation introduced a better understanding of the effects of NG composition on conventional dual-fuel and RCCI combustion modes at a wide range of engine load conditions. The results demonstrated that changes in MN do not necessarily require modifications in engine calibration if variations in fuel conversion efficiency are within an acceptable range and additional engine-out emissions can be managed by the aftertreatment system. Nevertheless, this work showed that the advanced RCCI operation with LIVC significantly reduced NO<sub>x</sub> and CH<sub>4</sub> emissions while achieving higher peak combustion efficiency (98.9% vs 97.2%) and net indicated efficiency (45.2% vs 42.3%) than the conventional dual-fuel combustion. These research findings can be used to support the optimisation and development of high-efficiency and clean dual-fuel engines, potentially helping to minimise their impact on air pollution and climate change.

### Acknowledgement

The authors also would like to acknowledge Dr. Ian May (General Motors) for all the advice given during this research work and Nina Liem (Shell/CRI) for the technical support during the selection of the NG fuels.



### Declaration of conflicting interests

The author(s) declared no potential conflicts of interest with respect to the research, authorship, and/or publication of this article.

### Funding

The author(s) disclosed receipt of the following financial support for the research, authorship, and/or publication of this article: This research work was conducted within the scope of the DUET project (Heavy Duty Dual Fuel Demonstrator Engine Achieving Future EU Emissions Compliance with 23% Carbon Reduction), part-funded by the Innovate UK, project number 102660.

### ORCID iDs

Vinicius B Pedrozo  <https://orcid.org/0000-0002-0836-2693>  
Xinyan Wang  <https://orcid.org/0000-0002-1988-3742>

### References

1. Delgado O and Muncrief R. Assessment of heavy-duty natural gas vehicle emissions: implications and policy recommendations. White paper, 2015.
2. Ran Z, Hariharan D, Lawler B, et al. Exploring the potential of ethanol, CNG, and syngas as fuels for lean spark-ignition combustion: an experimental study. *Energy* 2020; 191: 116520.
3. Leach F, Kalghatgia G, Stonea R, et al. The scope for improving the efficiency and environmental impact of internal combustion engines. *Transp Eng* 2020; 1: 100005.
4. May I, Pedrozo V, Zhao H, et al. Characterization and potential of premixed dual-fuel combustion in a heavy duty natural gas/diesel engine. SAE technical paper 2016-01-0790, 2016. DOI: 10.4271/2016-01-0790.
5. Kokjohn SL, Hanson RM, Splitter DA, et al. Fuel reactivity controlled compression ignition (RCCI): a pathway to controlled high-efficiency clean combustion. *Int J Engine Res* 2011; 12(3): 209–226.
6. Pedrozo VB, May I, Guan W, et al. High efficiency ethanol-diesel dual-fuel combustion: a comparison against conventional diesel combustion from low to full engine load. *Fuel* 2018; 230: 440–451.
7. Intergovernmental Panel on Climate Change (IPCC). Climate Change 2014: Synthesis report. In: Core Writing Team, Pachauri and L.A. Meyer LA (eds) *Contribution of working groups I, II and III to the fifth assessment report of the intergovernmental panel on climate change*. Geneva, Switzerland: IPCC. 2014, 151 pp.
8. Frankl S, Gleis S, Karmann S, et al. Investigation of ammonia and hydrogen as CO<sub>2</sub>-free fuels for heavy duty engines using a high pressure dual fuel combustion process. *Int J Engine Res* 2020; 1468087420967873. DOI: 10.1177/1468087420967873.
9. Stettler ME, Midgley WJB, Swanson JJ, et al. Greenhouse gas and noxious emissions from dual fuel diesel and natural gas heavy goods vehicles. *Environ Sci Technol* 2016; 50(4): 2018–2026.
10. Economic Commission for Europe of the United Nations (UN/ECE), Regulation No. 49 – uniform provisions concerning the measures to be taken against the emission of gaseous and particulate pollutants from compression-ignition engines and positive ignition engines for use in vehicles. *OJEU* 2010; L229/1.
11. The European Parliament and the Council of the European Union, Regulation (EC) No. 595/2009. *OJEU* 2009.
12. The European Parliament and the Council of the European Union, Commission Regulation (EU) No. 582/2011. *OJEU* 2011.
13. Smith I, Chiu J, Bartley G, et al. Achieving fast catalyst light-off from a heavy-duty stoichiometric natural gas engine capable of 0.02 g/bhp-hr NO<sub>x</sub> emissions. SAE technical paper 2018-01-1136, 2018. DOI: 10.4271/2018-01-1136.
14. International Group of LNG Importers (GIIGNL). GIIGNL annual report 2018, 2018. Groupe International des Importateurs de Gaz Naturel Liquéfié (GIIGNL).
15. Benajes J, García A, Monsalve-Serrano J, et al. Achieving clean and efficient engine operation up to full load by combining optimized RCCI and dual-fuel diesel-gasoline combustion strategies. *Energy Convers Manage* 2017; 136: 142–151.

16. Guan W, Pedrozo VB, Zhao H, et al. Miller cycle combined with exhaust gas recirculation and post-fuel injection for emissions and exhaust gas temperature control of a heavy-duty diesel engine. *Int J Engine Res* 2019; 21: 146808741983001.
17. Guan W, Pedrozo V, Zhao H, et al. Variable valve actuation-based combustion control strategies for efficiency improvement and emissions control in a heavy-duty diesel engine. *Int J Engine Res* 2020. 21(4): 578–591.
18. Pedrozo VB, May I and Zhao H, Exploring the mid-load potential of ethanol-diesel dual-fuel combustion with and without EGR. *Appl Energy* 2017; 193: 263–275.
19. Ahmad Z, Kaario O, Cheng Q, et al. Impact of ethane enrichment on diesel-methane dual-fuel combustion. SAE technical paper 2020-01-0305, 2020. DOI: 10.4271/2020-01-0305.
20. Belgiorno G, Di Blasio G and Beatrice C. Parametric study and optimization of the main engine calibration parameters and compression ratio of a methane-diesel dual fuel engine. *Fuel* 2018; 222: 821–840.
21. Pedrozo VB, May I, Thompson DM, et al. Potential of internal EGR and throttled operation for low load extension of ethanol–diesel dual-fuel reactivity controlled compression ignition combustion on a heavy-duty engine. *Fuel (Guildford)* 2016; 179: 391–405.
22. Pedrozo V, May I and Zhao H. Characterization of low load ethanol dual-fuel combustion using single and split diesel injections on a heavy-duty engine. SAE technical paper 2016-01-0778, 2016. DOI: 10.4271/2016-01-0778.
23. Desantes JM, Benajes J, García A, et al. The role of the in-cylinder gas temperature and oxygen concentration over low load reactivity controlled compression ignition combustion efficiency. *Energy* 2014; 78: 854–868.
24. Liu H, Tang Q, Ran X, et al. Optical diagnostics on the reactivity controlled compression ignition (RCCI) with micro direct-injection strategy. *Proc Combust Inst* 2019; 37(4): 4767–4775.
25. Yousefi A, Guo H and Birouk M. An experimental and numerical study on diesel injection split of a natural gas/diesel dual-fuel engine at a low engine load. *Fuel* 2018; 212: 332–346.
26. Yousefi A, Guo H, Birouk M, et al. On greenhouse gas emissions and thermal efficiency of natural gas/diesel dual-fuel engine at low load conditions: coupled effect of injector rail pressure and split injection. *Appl Energy* 2019; 242: 216–231.
27. Pedrozo VB, May I, Lanzanova T, et al. The effective use of ethanol for GHG emissions reduction in a dual-fuel engine. In: Siebenpfeiffer W. (eds) *Heavy-Duty-, On- and Off-Highway-Motoren* 2018. Springer Vieweg, Wiesbaden, 2019, [https://doi.org/10.1007/978-3-658-25889-4\\_11](https://doi.org/10.1007/978-3-658-25889-4_11)
28. Dahodwala M, Joshi S, Koehler E, et al. Investigation of diesel-CNG RCCI combustion at multiple engine operating conditions. SAE technical paper 2020-01-0801, 2020. DOI: 10.4271/2020-01-0801.
29. Benajes J, García A, Monsalve-Serrano J, et al. Fuel consumption and engine-out emissions estimations of a light-duty engine running in dual-mode RCCI/CDC with different fuels and driving cycles. *Energy* 2018; 157: 19–30.
30. Ren S, Wang B, Zhang J, et al. Application of dual-fuel combustion over the full operating map in a heavy-duty multi-cylinder engine with reduced compression ratio and diesel oxidation catalyst. *Energy Convers Manage* 2018; 166: 1–12.
31. García A, Monsalve-Serrano J, Villalta D, et al. Fuel sensitivity effects on dual-mode dual-fuel combustion operation for different octane numbers. *Energy Convers Manage* 2019; 201: 112137.
32. Karavalakis G, Hajbabaie M, Jiang Y, et al. Regulated, greenhouse gas, and particulate emissions from lean-burn and stoichiometric natural gas heavy-duty vehicles on different fuel compositions. *Fuel* 2016; 175: 146–156.
33. GIIGNL. *Rollover in LNG storage tanks*. Summary Report by the GIIGNL Technical Study Group on the Behaviour of LNG in Storage, 2015. Groupe International des Importateurs de Gaz Naturel Liquéfié (GIIGNL), Neuilly-sur-Seine, France.
34. Van Essen M, Gersen S, Van Dijk G, et al. Methane number: a key parameter for LNG use as vehicle fuel. DNV GL paper, 2017.
35. Bommisetty H, Liu J, Kooragayala R, et al. Fuel composition effects in a CI engine converted to SI natural gas operation. SAE technical paper 2018-01-1137, 2018. DOI: 10.4271/2018-01-1137.
36. International Group of Liquefied Natural Gas Importers (GIIGNL). Position paper on the impact of including methane number in natural gas regulation, 2014.
37. Giesekeing B and Brown AS. Novel algorithm for calculating the methane number of liquefied natural gas with defined uncertainty. *Fuel* 2016; 185: 932–940.
38. Eilts P and Klare L. Investigations on the Determination of the Service Methane Number of LNG. 2018. SAE Technical Paper 2018-01-1143. DOI: 10.4271/2018-01-1143.
39. Stone R. *Introduction to internal combustion engines* 4th ed. Hampshire, UK: Macmillan International Higher Education, 2012.
40. Naber JD, Siebers DL, Di Julio SS, et al. Effects of natural gas composition on ignition delay under diesel conditions. *Combust Flame* 1994; 99(2): 192–200.
41. Karavalakis G, Gysel N, Hajbabaie M, et al. Influence of different natural gas compositions on the regulated emissions, aldehydes, and particle emissions from a transit bus. SAE technical paper 2013-01-1137, 2013. DOI: 10.4271/2013-01-1137.
42. Kramer U, Lorenz T, Hofmann C, et al. Methane number effect on the efficiency of a downsized, dedicated, high performance compressed natural gas (CNG) direct injection engine. SAE technical paper 2017-01-0776, 2017. DOI: 10.4271/2017-01-0776.
43. Liu J and Dumitrescu CE. Numerical investigation of methane number and Wobbe index effects in lean-burn natural gas spark-ignition combustion. *Energy Fuels* 2019; 33(5): 4564–4574.
44. Reitz RD and Duraisamy G. Review of high efficiency and clean reactivity controlled compression ignition (RCCI) combustion in internal combustion engines. *Prog Energy Combust Sci* 2015; 46: 12–71.
45. Van Alstine DG, Montgomery DT, Callahan TJ, et al. Ability of the methane number index of a fuel to predict rapid combustion in heavy duty dual fuel engines for North American locomotives. In: *Proceedings of the ASME 2015 internal combustion engine division fall technical conference*, Volume 1: Large Bore Engines, Fuels, Advanced Combustion. Houston, Texas, USA, 8–11 November 2015. V001T02A010. ASME. DOI: 10.1115/ICEF2015-1119.

46. Wu Z, Rutland CJ and Han Z, Numerical evaluation of the effect of methane number on natural gas and diesel dual-fuel combustion. *Int J Engine Res* 2018; 20(4): 405–423.
47. Kakaee A, Rahnema P and Paykani A. Influence of fuel composition on combustion and emissions characteristics of natural gas/diesel RCCI engine. *J Nat Gas Sci Eng* 2015; 25: 58–65.
48. Pedrozo VB and Zhao H. Improvement in high load ethanol-diesel dual-fuel combustion by Miller cycle and charge air cooling. *Appl Energy* 2018; 210: 138–151.
49. Guan W, Wang X, Zhao H, et al. Exploring the high load potential of diesel-methanol dual-fuel operation with Miller cycle, exhaust gas recirculation, and intake air cooling on a heavy-duty diesel engine. *Int J Engine Res* 2020; 146808742092677. DOI: 10.1177/14680874 20926775.
50. Boronat V, Splitter D and Chuahy FDF. Achieving diesel-like efficiency in a high stroke-to-bore ratio DISI engine under stoichiometric operation. SAE technical paper 2020-01-0293, 2020. DOI: 10.4271/2020-01-0293.
51. He X, Durrett RP and Sun Z, Late intake valve closing as an emissions control strategy at Tier 2 Bin 5 engine-out NOx level. *SAE Int J Engines* 2009; 1(1): 427–443.
52. Heywood JB. *Internal combustion engine fundamentals*. New York: McGraw-Hill Education, 1988.
53. Ickes A, Hanson R and Wallner T. Impact of effective compression ratio on gasoline-diesel dual-fuel combustion in a heavy-duty engine using variable valve actuation. SAE technical paper 2015-01-1796, 2015. DOI: 10.4271/2015-01-1796.
54. Naber JD, Siebers D, Caton J, et al. Natural gas auto-ignition under diesel conditions: experiments and chemical kinetic modeling. SAE technical paper 942034, 1994. DOI: <https://doi.org/10.4271/942034>.
55. Healy D, Curran HJ, Simmie JM, et al. Methane/ethane/propane mixture oxidation at high pressures and at high, intermediate and low temperatures. *Combust Flame* 2008; 155(3): 441–448.
56. Gibbs GJ and Calcote HF. Effect of molecular structure on burning velocity. *J Chem Eng Data* 1959; 4(3): 226–237.
57. DNV GL. PKI methane number calculator for LNG. <https://www.dnvgl.com/oilgas/natural-gas/fitness-for-purpose-of-lng-pki-methane-number-calculator.html> (accessed 5 February 2018).
58. Wärtsilä. Wärtsilä methane number calculator. <https://www.wartsila.com/marine/build/gas-solutions/methane-number-calculator> (accessed 5 February 2018).
59. MWM. MWM MN calculation program. <https://www.euromot.eu/wp-content/uploads/2019/07/MWM-MN-Code-for-distribution-2016-04-22.zip> (accessed 5 February 2018).
60. Westport. Fuel quality calculator. <https://www.cumminswestport.com/fuel-quality-calculator> (accessed 5 February 2018).
61. Amirante R, Distaso E, Tamburrano P, et al. Laminar flame speed correlations for methane, ethane, propane and their mixtures, and natural gas and gasoline for spark-ignition engine simulations. *Int J Engine Res* 2017; 18(9): 951–970.
62. Rochussen J and Kirchen P. Characterization of reaction zone growth in an optically accessible heavy-duty diesel/methane dual-fuel engine. *Int J Engine Res* 2019; 20(5): 483–500.
63. Caton JA. Maximum efficiencies for internal combustion engines: thermodynamic limitations. *Int J Engine Res* 2017; 19(10): 1005–1023.
64. Worth DJ, Stettler MEJ, Dickinson P, et al. Characterization and evaluation of methane oxidation catalysts for dual-fuel diesel and natural gas engines. *Emission Control Sci Technol*. 2016; 2(4): 204–214.
65. Zammit JP, McGhee MJ, Shayler PJ, et al. The effects of early inlet valve closing and cylinder disablement on fuel economy and emissions of a direct injection diesel engine. *Energy* 2015; 79: 100–110.